7. Gilday DL, Kellam J. Indium-111-DTPA evaluation of CSF diversionary shunts in children. *J Nucl Med* 1973;14:920–923.
8. Graham P, Howman-Giles R, Johnston I, Besser M. Evaluation of CSF shunt patency by means of technetium-99m DTPA. *J Neurosurg* 1982;57:262–266.
9. Harbert J, Haddad D, McCullough D. Quantitation of cerebrospinal fluid shunt flow. *Radiology* 1974;112:379–387.
10. Hayden PW, Rudd TG, Dizmang D, Loeser JD, Shurtleff DB. Evaluation of surgically treated hydrocephalus by radionuclide clearance studies of the cerebrospinal fluid shunt. *Dev Med Child Neurol* 1974;16:72–78.
11. Hayden PW, Rudd TG, Shurtleff DB. Combined pressure-radionuclide evaluation of suspected cerebrospinal fluid shunt malfunction: a seven-year clinical experience. *Pediatrics* 1980;66:679–684.
12. James AE, DeBlanc HJ, DeLand FH, Matthews ES. Refinements in cerebrospinal fluid diversionary shunt evaluation by cisternography. *Am J Roentgenol Radium Ther Nucl Med* 1972;115:766–773.
13. Rudd TG, Shurtleff DB, Loeser JD, Nelp WB. Radionuclide assessment of cerebrospinal fluid shunt function in children. *J Nucl Med* 1973;14:683–686.
14. Sty JR, D'Souza BJ, Daniels D. Nuclear anatomy of diversionary central nervous system shunts in children. *Clin Nucl Med* 1978;3:271–275.
15. Uvebrant P, Sixt R, Bjure J, Roos A. Evaluation of cerebrospinal fluid shunt function in hydrocephalic children using ^{99m}Tc-DTPA. *Child's Nerv Syst* 1992;8:76–80.
16. Brisman R, Schneider S, Carter S. Subarachnoid infusion and shunt function: technical note. *J Neurosurg* 1973;38:379–381.
17. Matin P, Goodwin DA, DeNardo GL. Cerebrospinal fluid scanning and ventricular shunts. *Radiology* 1970;94:435–438.
18. Brereton RJ. The value of an ultrasonic flowmeter in assessing the function of CSF shunts. *J Pediatr Surg* 1980;15:68–73.
19. Flitter MA, Buchheit WA, Murtagh F, Lapayowker MS. Ultrasound determination of cerebrospinal fluid shunt patency: technical note. *J Neurosurg* 1975;42:728–730.
20. Chiba Y, Yuda K. Thermosensitive determination of CSF shunt patency with a pair of small disc thermistors. *J Neurosurg* 1980;52:700–704.
21. Go KG, Lakke JPWF, Beks JWF. A harmless method for the assessment of the patency of ventriculoatrial shunts in hydrocephalus. *Dev Med Child Neurol* 1968;16:100–106.
22. Atkinson JR, Folz EL. Intraventricular "RISA" as diagnostic aid in pre- and postoperative hydrocephalus. *J Neurosurg* 1962;19:159–166.
23. Bell RL. Isotope transfer in the diagnosis and treatment of hydrocephalus. *Int J Applied Radiat* 1959;5:89–93.
24. Kagen A, Tsuchiya G, Patterson V, Sugar O. Test for patency of ventriculovascular shunt for hydrocephalus with radioactive iodinated serum albumin. *J Neurosurg* 1963;20:1025–1028.
25. Epstein F, Lapras C, Wisoff JH. "Slit-ventricle syndrome:" etiology and treatment. *Pediatr Neurosci* 1988;14:5–10.

Hypoperfusion in the Limbic System and Prefrontal Cortex in Depression: SPECT with Anatomic Standardization Technique

Hiroshi Ito, Ryuta Kawashima, Shuichi Awata, Shuichi Ono, Kazunori Sato, Ryoui Goto, Masamichi Koyama, Mitsumoto Sato and Hiroshi Fukuda

Department of Nuclear Medicine and Radiology, Division of Brain Sciences, Institute of Development, Aging and Cancer, Tohoku University, and Department of Psychiatry, Tohoku University School of Medicine, Sendai, Japan

Depression is a common psychiatric illness, and several reports have described cerebral blood flow (CBF) abnormalities on SPECT studies in affected patients. However, because region of interest analyses were used to determine significant CBF changes in these studies, there were methodological limitations. Therefore, we investigated CBF distribution abnormalities in depression on a pixel-by-pixel basis using SPECT and an anatomic standardization technique that has been commonly used for PET activation studies. **Methods:** Eleven patients with unipolar depression, six patients with bipolar depression and nine age-matched normal control subjects underwent HMPAO brain SPECT studies. The radioactivities of SPECT images for each subject were globally normalized to 100 counts/pixel. Then, each SPECT image was transformed for standard brain anatomy using a computerized Human Brain Atlas system. For each group, the mean and variance images were calculated from the standardized anatomic SPECT images, and group comparisons were performed on a pixel-by-pixel basis. **Results:** Significant decreases in CBF in the prefrontal cortices, limbic systems and paralimbic areas were observed in both depression groups compared with the normal control group. **Conclusion:** Decreases in CBF in these regions may be related to impaired attention as well as cognitive and emotional responses, which have been recognized as usual symptoms in depression. The anatomic standardization technique promises to be useful for group comparison analysis of brain SPECT on a pixel-by-pixel basis for individual neurological and psychiatric diseases.

Key Words: depression; SPECT; anatomic standardization; limbic system; prefrontal cortex

J Nucl Med 1996; 37:410–414

Depression is a common psychiatric illness (*1*), and many reports have described associated cerebral blood flow (CBF) and metabolism abnormalities on SPECT and PET studies in affected patients (*2–12*). Several investigators have described CBF decreases in the paralimbic regions (*2*); left prefrontal and both temporal regions (*3*); selective frontal, central, superior temporal and anterior parietal regions (*4*); whole brain (*5*); and left cerebral hemisphere (*6*) in patients with different types of depression. However, a lack of any significant changes in CBF in depression has also been reported (*7*). Decreased glucose metabolism in the left dorsal anterolateral prefrontal cortex may occur in some types of depression (*8,9*). The use, however, of region of interest analyses to determine significant CBF changes in these studies introduced limitations in the sensitivity of the imaging approaches (*13*).

Fox et al. (*13*) reported that intersubject averaging of PET images, a technique requiring transformation of brain images of individual subjects into a standard brain shape and size in three dimensions (*anatomic standardization*), allows enhanced detection of focal brain responses. The anatomic standardization technique also permits group comparisons between normal control subjects and patients on a pixel-by-pixel basis (*14,15*). Recent reports describe CBF abnormalities on PET studies with anatomic standardization in patients with depression (*11,12*). These studies reported the finding of hypoperfusion in the left anterior cingulate and left dorsolateral prefrontal cortex (*11*). Assessment of brain SPECT abnormalities using the anatomic standardization technique has also been proposed (*16*).

Recently, Roland et al. (*17*) developed a new computerized human brain atlas (HBA) system that transforms the brain anatomic structures of subjects into a standard anatomic format using linear and nonlinear parameters. The purpose of the

Received Feb. 22, 1995; revision accepted Jun. 7, 1995.

For correspondence or reprints contact: Ryuta Kawashima, MD, Department of Nuclear Medicine and Radiology, Division of Brain Sciences, Institute of Development, Aging and Cancer, Tohoku University, 4-1 Seiryo-Machi, Aoba-Ku, Sendai, Japan 980.

TABLE 1
Profiles of 17 Patients with Depression

Parameter	Unipolar (n = 11)	Bipolar (n = 6)
Sex (M/F)	4/7	5/1
Age (yr)	66.6 ± 7.1	66.7 ± 5.8
Hamilton Rating Scale	10.6 ± 7.9	9.8 ± 9.6
Mini-Mental State	26.1 ± 4.7	24.4 ± 3.8
Medication		
Tricyclic antidepressants	11/11	1/6
Minor tranquilizers	5	5
Major tranquilizers	4	5
Lithium carbonate	0	3

Values are mean ± s.d. or number of patients.

present study was to estimate CBF abnormalities on brain SPECT by group comparison of patients with depression with normal control subjects, using this HBA system.

MATERIALS AND METHODS

Subjects

Eleven patients with unipolar depression (Unipolar) (mean [±s.d.] age 66.6 ± 7.1 yr, range 59–77 yr), six patients with bipolar depression (Bipolar) (mean age 66.7 ± 5.8 yr, range 61–77 yr) and nine age-matched normal control subjects with no sign or history of medical or neurological disease and normal findings on x-ray computed tomography (CT) of the brain (control) (mean age 65.7 ± 10.5 yr, range 50–81 yr) underwent SPECT studies. Clinical diagnosis of unipolar and bipolar depression was made by psychiatrists according to DSM-IV criteria (*18*). Patients with unipolar and bipolar depression were diagnosed as having DSM-IV Major Depressive Disorder, Recurrent (296.3) and Bipolar I Disorder, Most Recent Episode Depressed (296.5), respectively. No patient had abnormal findings on brain x-ray CT, neurological deficits or cerebrovascular risk factors (i.e., hypertension, diabetes or ischemic heart disease). All patients were right-handed. Exclusion criteria were a past or present history of neurological or other psychiatric disease; drug or alcohol abuse, or both; and use of cerebral metabolic activator, vasodilator or dopamine-agonist medications and electroconvulsive therapy within 6 mo. All patients were examined using the Hamilton Rating Scale for Depression (*19*) and Mini-Mental State Examination (*20*) just before SPECT studies (Table 1). All patients had had at least two prior episodes of depression, and all were in a state of partial remission with antidepressant medications (Table 1) and had residual symptoms at SPECT study. Exclusion from neurodegenerative disorders, such as frontotemporal dementia, was confirmed by a significant lessening of cognitive impairment at clinical examinations during a follow-up period of 1–2 yr after initial SPECT studies. Written informed consent was obtained from each subject.

SPECT

SPECT scans were obtained 5–10 min after an intravenous bolus injection of 925–1110 MBq ^{99m}Tc-labeled hexamethylpropylene-amineoxime (HMPAO) as a CBF tracer (*21,22*). During injection of HMPAO, subjects were in a supine position with eyes closed. One SPECT scanner (SPECT-2000H, Hitachi Medico Corp., Tokyo, Japan) (*23*), a four-head rotating gamma camera with in-plane and axial resolutions of 8-mm FWHM, was used for all measurements. The SPECT scan protocol acquired 64 projections at 20 sec (20 sec × four-head camera = total 80 sec) per projection, with 360° rotation of the camera. Image reconstruction was performed by filtered backprojection using a Butterworth filter (*24*), and attenuation correction was made numerically by assuming an ellipitic object shape for each slice and a uniform attenuation coefficient (0.1 cm^{-1}) (*25,26*). Correction for scattered photons was not performed. Image slices were arranged parallel to the orbitomeatal line and obtained for 8-mm intervals through the whole brain. After SPECT measurements, x-ray CT scans were obtained with the same slices as for SPECT images in all subjects.

Data Analysis

Each subject's SPECT and x-ray CT images were transferred to a Unix Workstation, Sparc-Sun 10, where all data analyses were performed.

Anatomic Standardization of SPECT Images. SPECT images for each subject were transformed into the standard brain size and shape using the HBA system (*17*). The anatomic structures of the computerized standard brain atlas (i.e., contour of the brain, main sulci and ventricles) were fitted interactively to each subject's x-ray CT images using both linear and nonlinear parameters in three-dimensional space. These parameters were subsequently used to transform each subject's SPECT image into the standard atlas form. Each subject's x-ray CT images were also transformed using same parameters for confirmation of correct transformation into the standard brain atlas form.

Statistical Analysis. After the anatomic standardization procedure, all subjects' SPECT images had the same anatomic brain format. The radioactivities of each SPECT image were globally normalized to 100 counts/pixel using whole-brain radioactivities. Then, the mean and variance images of brain radioactivities were calculated pixel by pixel for each group of subjects. From these calculations, descriptive three-dimensional t-images of control minus unipolar and control minus bipolar were calculated. In the descriptive t-images, t-values over 2.10 and 2.16 were considered statistically significant, corresponding to a significance level of $p < 0.05$ (after Bonferroni correction for multiple comparisons) for control minus unipolar or control minus bipolar.

RESULTS

The mean SPECT images for patients with unipolar and bipolar depression and normal control subjects are shown in Figure 1. The t-images of control minus unipolar and control minus bipolar, illustrating areas of significant changes are shown in Figures 2 and 3, respectively. Significant decreases in CBF in the unipolar depression group compared with the normal control group were observed in the following regions: the anterior aspect of the superior, middle and inferior frontal gyri of the bilateral hemispheres; the right anterior cingulate region; the anterior aspect of the left superior temporal gyrus; the posterior aspect of the left superior temporal gyrus; and anterior part of the insular cortex of the bilateral hemispheres ($p < 0.05$) (Fig. 2, Table 2). Significant decreases in CBF in the bipolar depression group were observed in following regions: the anterior aspect of the superior and middle frontal gyri of the bilateral hemispheres, the right anterior cingulate region, the anterior aspect of the left superior temporal gyrus, the left angular gyrus, the left lingual gyrus and the anterior part of the insular cortex of the bilateral hemispheres ($p < 0.05$) (Fig. 3, Table 2).

DISCUSSION

Our anatomic standardization technique allows intersubject averaging of SPECT images and group comparison analyses on a pixel-by-pixel basis. Enhanced detection of focal CBF changes in the present series could therefore be made. This technique should also prove useful for group comparison analyses of brain SPECT images from patients with other neurological and psychiatric diseases.

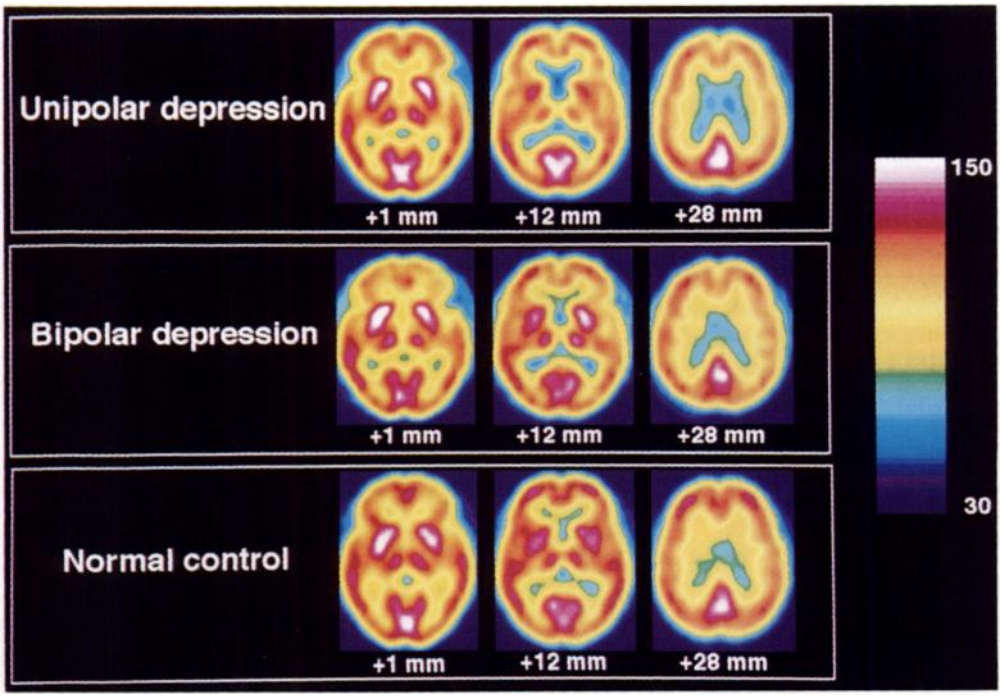

FIGURE 1. Mean anatomically standardized SPECT images from patients with unipolar and bipolar depression and normal control subjects. Image slices were transverse +1, +12 and +28 mm relative to the anteroposterior commissure line. The anterior is at the top of the image, and the subjects' right is at the left. The radioactivities of each SPECT image were globally normalized to 100 counts/pixel. Scale maximum and minimum values are 150 and 30 counts/pixel, respectively.

The biologic cause of depression is unknown, despite the many biochemical investigations that have been reported (*27–30*). In the present study, both unipolar and bipolar depression groups demonstrated significant CBF decreases, observed bilaterally in the prefrontal cortices, the limbic system and the paralimbic areas. These findings are consistent with several previous reports (*2,3,8,9,11*).

It has been reported that the limbic system, particularly the anterior cingulate, becomes activated in a special form of attention in humans. A role for this region in attentional processing has therefore been considered (*31,32*). Impaired attention is a usual symptom in patients with depression, and it could be argued that hypoperfusion in the anterior cingulate might be related to this impaired attention. A role for the anterior cingulate has also been reported in modulation of emotion in monkeys (*33*) and at the interface between attention and emotion in rats and cats (*34*). Depression is the major illness of emotion, and the most characteristic symptom is a depressed mood. Therefore, hypoperfusion in the anterior cingulate might also be related to emotional impairment, although this would contradict previous findings in humans that this brain region does not create emotions (*32,35*).

In the present study, decreases in CBF were also observed in the anterior aspect of the left temporal lobe and the anterior part of the insular cortex of the bilateral hemispheres. These areas are included in the paralimbic area. The significance of the anterior part of the insular cortex has been investigated in terms of cognitive and learning function in humans (*36*) and monkeys (*37*). Cognitive impairments are often observed in patients with depression, particularly elderly patients with "pseudodementia" (*38*). The patients with depression in the present study were all elderly, and several had cognitive impairment that was indicated by a low score on the Mini-Mental State Examination (Table 1). Therefore, hypoperfusion in the anterior part of the insular cortex might indeed be related to cognitive and learning impairment. In addition, CBF decreases in the left anterior

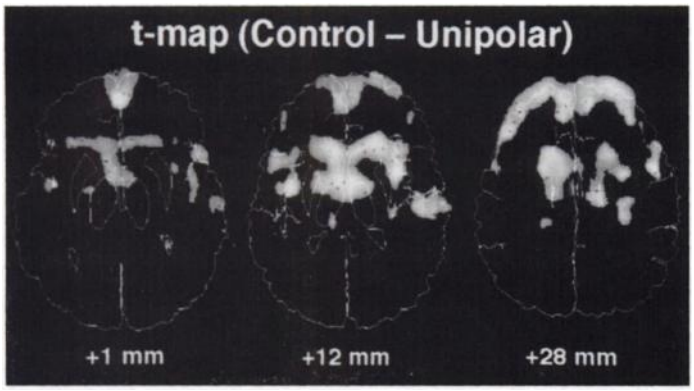

FIGURE 2. The t-image of control minus unipolar illustrating the areas with t-values over 2.10 ($p < 0.05$). Significant decreases in unipolar CBF were observed in the following regions: the anterior aspect of the superior, middle and inferior frontal gyri of the bilateral hemispheres; the right anterior cingulate region; and the anterior part of the insular cortex of the bilateral hemispheres. Image slices were transverse +1, +12 and +28 mm relative to the anteroposterior commissure line. The anterior is at the top of the image, and the subjects' right is at the left. Scale maximum and minimum values are 5 and 0, respectively.

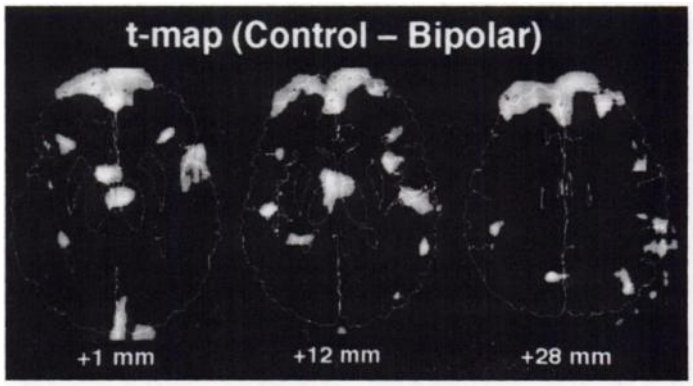

FIGURE 3. The t-image of control minus bipolar illustrating the areas with t-values over 2.16 ($p < 0.05$). Significant decreases in bipolar CBF were observed in the following regions: the anterior aspect of the superior and middle frontal gyri of the bilateral hemispheres, the right anterior cingulate region and the anterior part of the insular cortex of the bilateral hemispheres. Image slices were transverse +1, +12 and +28 mm relative to the anteroposterior commissure line. The anterior is at the top of the image, and the subjects' right is at the left. Scale maximum and minimum values are 5 and 0, respectively.

TABLE 2
Coordinates of Pixels Where Significant CBF Changes Were Identified

Location	Coordinate*			t-value†	
	x	y	z	Unipolar	Bipolar
Anterior cingulate	−3	48	1	2.75	2.53
Insular cortex	−36	−4	12	4.21	—
	−31	20	4	—	3.09
	33	10	12	4.21	4.16
Prefrontal cortex	−20	56	28	3.14	3.05
	27	55	28	3.17	3.08

*Coordinates x, y, z are in milliliters, measured from the anterior commissure, corresponding to the atlas of Talairach and Tournoux (*60*). Coordinates are given in the order x (width), y (anterior-posterior) and z (height).

†Unipolar and bipolar t-values correspond to control minus unipolar and control minus bipolar, respectively (see text for explanation).

medial prefrontal cortex have been reported in patients with depression versus those without cognitive impairment (*12*). It has also been reported that paralimbic area activities are related to emotional changes in humans (*32*) and in rats (*39*).

The prefrontal cortex is activated by selective attention (*40,41*) as well as visual (*42*) and auditory (*43*) discrimination and recognition in humans, and these findings suggest the functions of the prefrontal cortex (*32*). It has also been reported that some of the roles of the prefrontal cortex are involved in short-term memory in monkeys (*44–48*) and motivation in rats (*49*). The usual symptoms of depression (i.e., attentional and cognitive impairment, depressed mood and inhibition of thought) might be related to hypoperfusion in the prefrontal cortex. In addition, connections between the rostralmost part of the cingulate gyrus and the lateral prefrontal cortex have been confirmed in monkeys (*50*) and, therefore, dysfunction of the prefrontal cortex and the anterior cingulate might be reciprocally related.

In the SPECT study, all patients were in a state of partial remission of depression according to DSM-IV, as indicated by relatively low scores on the Hamilton Rating Scale for Depression compared with scores of patients with depression in previous studies (Table 1). However, similar results (i.e., hypoperfusion in the anterior cingulate and prefrontal cortex) were obtained. All patients had two or more previous major depressive episodes. Despite antidepressant treatment for recent major depressive episodes, they were in a state of partial remission and had residual symptoms. In addition, they all were elderly and had some degree of treatment resistance. It might thus be possible to argue that elderly patients with refractory depression show CBF abnormalities similar to those in patients in the severely ill phases of depression, even though they are in a state of partial remission with residual symptoms.

Antidepressant medication would affect these CBF abnormalities. In the present study, the doses of antidepressant agents were very small compared with doses in common use, and therefore it was considered that the depressed mental state was the main source of the CBF abnormalities. However, a controlled study of the effects of medication would be required to confirm this conclusion.

The anatomic standardization technique allows for group comparison analysis of brain SPECT on a pixel-by-pixel basis but some technical errors may exist. The standard brain used in the HBA system was obtained from 20–30-yr-old healthy subjects (*17*). In the present study, the subjects were 66–67 yr old on average. Because our subjects' brains showed slight atrophy compared with the standard brain, misregistrations might have occurred with transformation to the standard brain format. For example, the size of the ventricles, including the lateral, third and fourth ventricles, in the subjects' brains were slightly different from that of the standard brain. Therefore, we did not estimate CBF changes in the periventricular structures.

Technetium-99m-HMPAO, the tracer used in the present study, shows backdiffusion from the brain (*51–54*) and limited first-pass extraction fraction (*55,56*). These features must cause the nonlinearity of brain radioactivities compared with that of the true CBF. Underestimation of CBF has been argued to occur, especially in high CBF regions (*55,56*), and a linearization method for CBF estimation using HMPAO has therefore been proposed (*51*). However, because this linearization method might enhance errors in SPECT data, we did not use it in the present study.

In addition, scattered photons not removed in this study could have caused errors in SPECT estimation of CBF (i.e., significant CBF changes were observed in areas outside the brain parenchyma) (Figs. 2 and 3). These errors should be corrected in the future (*57–59*).

CONCLUSION

The present investigation of abnormalities in CBF distribution in cases of unipolar and bipolar depression on a pixel-by-pixel basis using SPECT and the anatomic standardization technique revealed decreased CBF in the prefrontal cortices, limbic systems and paralimbic areas of both depression groups compared with that in age-matched control subjects. These findings indicate that dysfunction of these regions might be related to the attentional, cognitive and emotional impairments that are recognized as usual symptoms in depression. The anatomic standardization technique should prove useful for group comparison analyses of brain SPECT on a pixel-by-pixel basis for other neurological and psychiatric diseases.

ACKNOWLEDGMENTS

We are greatly indebted to the staff of the Institute of Development, Aging and Cancer, Tohoku University and in particular, Mr. Tachio Sato for performing the SPECT scans. This study was supported by a Grant-in-Aid for Scientific Research (05454297) from the Japanese Ministry of Education, Science and Culture.

REFERENCES

1. Robins LN, Helzer JE, Weissman MM, et al. Lifetime prevalence of specific psychiatric disorders in three sites. *Arch Gen Psychiatry* 1984;41:949–958.
2. Mayberg HS, Lewis PJ, Regenold W, Wagner HN Jr. Paralimbic hypoperfusion in unipolar depression. *J Nucl Med* 1994;35:929–934.
3. Yazici KM, Kapucu O, Erbas B, Varoglu E, Gulec C, Bekdik C. Assessment of changes in regional cerebral blood flow in patients with major depression using the ^{99m}Tc-HMPAO single photon emission tomography method. *Eur J Nucl Med* 1992;19:1038–1043.
4. Sackeim HA, Prohovnik I, Moeller JR, et al. Regional cerebral blood flow in mood disorders. *Arch Gen Psychiatry* 1990;47:60–70.
5. Warren LR, Butler RW, Katholi CR, et al. Focal change in cerebral blood flow produced by monetary incentive during a mental mathematics task in normal and depressed subjects. *Brain Cogn* 1984;3:71–85.
6. Mathew RJ, Meyer JS, Francis DJ, et al. Cerebral blood flow in depression. *Am J Psychiatry* 1980;137:1449–1450.
7. Gur RE, Skolnick BE, Gur RC, et al. Brain function in psychiatric disorders. II. Regional cerebral blood flow in medicated unipolar depressives. *Arch Gen Psychiatry* 1984;41:695–699.
8. Baxter LR Jr, Schwartz JM, Phelps ME, et al. Reduction of prefrontal cortex glucose metabolism common to three types of depression. *Arch Gen Psychiatry* 1989;46:243–250.
9. Martinot JL, Hardy P, Feline A, et al. Left prefrontal glucose hypometabolism in the depressed state: a confirmation. *Am J Psychiatry* 1990;147:1313–1317.
10. Kumar A. Functional brain imaging in late-life depression and dementia. *J Clin Psychiatry* 1993;54:21–25.
11. Bench CJ, Friston KJ, Brown RG, Scott LC, Frackowiak RSJ, Dolan RJ. The anatomy of melancholia—focal abnormalities of cerebral blood flow in major depression. *Psychol Med* 1992;22:607–615.

12. Dolan RJ, Bench CJ, Brown RG, Scott LC, Friston KJ, Frackowiak RSJ. Regional cerebral blood flow abnormalities in depressed patients with cognitive impairment. *J Neurol Neurosurg Psychiatry* 1992;55:768–773.
13. Fox PT, Mintun MA, Reiman EM, Raichle ME. Enhanced detection of focal brain responses using intersubject averaging and change-distribution analysis of subtracted PET images. *J Cereb Blood Flow Metab* 1988;8:642–653.
14. Minoshima S, Koeppe RA, Frey KA, Ishihara M, Kuhl DE. Stereotactic PET atlas of the human brain: aid for visual interpretation of functional brain images. *J Nucl Med* 1994;35:949–954.
15. Minoshima S, Koeppe RA, Frey KA, Kuhl DE. Anatomic standardization: linear scaling and nonlinear warping of functional brain images. *J Nucl Med* 1994;35:1528–1537.
16. Houston AS, Kemp PM, Macleod MA. A method for assessing the significance of abnormalities in HMPAO brain SPECT images. *J Nucl Med* 1994;35:239–244.
17. Roland PE, Graufelds CJ, Wahlin J, et al. Human brain atlas: for high-resolution functional and anatomical mapping. *Human Brain Mapping* 1994;1:173–184.
18. American Psychiatric Association. *Diagnostic and statistical manual of mental disorders*, 4th ed. Washington, DC: American Psychiatric Association; 1994.
19. Hamilton M. A rating scale for depression. *J Neurol Neurosurg Psychiatry* 1960;23:56–62.
20. Folstein MF, Folstein SE, McHugh PR. "Mini-mental state": a practical method for grading the cognitive state of patients for the clinician. *J Psychiatr Res* 1975;12:189–198.
21. Sharp PF, Smith FW, Gemmell HG, et al. Technetium-99m HMPAO stereoisomers as potential agents for imaging regional cerebral blood flow: human volunteer studies. *J Nucl Med* 1986;27:171–177.
22. Neirinckx RD, Canning LR, Piper IM, et al. Technetium-99m d,l-HMPAO: a new radiopharmaceutical for SPECT imaging of regional cerebral blood perfusion. *J Nucl Med* 1987;28:191–202.
23. Kimura K, Hashikawa K, Etani H, et al. A new apparatus for brain imaging: four-head rotating gamma camera single-photon emission computed tomography. *J Nucl Med* 1990;31:603–609.
24. Budinger TF, Gullberg GT, Huesman RH. *Image reconstruction from projections.* New York: Springer-Verlag; 1979:197.
25. Chang LT. A method for attenuation correction in radionuclide computed tomography. *IEEE Trans Nucl Sci* 1978;25:638–643.
26. Chang LT. Attenuation correction and incomplete projection in single photon emission computed tomography. *IEEE Trans Nucl Sci* 1979;26:2780–2789.
27. Schildkraut JJ. The catecholamine hypothesis of affective disorders: A review of the supporting evidence. *Am J Psychiatry* 1965;122:509–522.
28. Van Praag HM, DeHaan S. Central serotonine metabolism and frequency of depression. *Psychiatry Res* 1979;1:219–224.
29. Gross-Iseseroff R, Dollon KA, Israeli M, Biegon A. Regionally selective increases in mu opioid receptor density in the brains of suicide victims. *Brain Res* 1990;530:312–316.
30. Mayberg HS, Robinson RG, Wong DF, et al. PET imaging of cortical S2 serotonin receptors after stroke: lateralized changes and relationship to depression. *Am J Psychiatry* 1988;145:937–943.
31. Pardo JV, Pardo PJ, Janer KW, Raichle ME. The anterior cingulate cortex mediates processing selection in the Stroop attentional conflict paradigm. *Proc Natl Acad Sci* 1990;87:256–259.
32. Roland PE. The frontal lobes and limbic system. In: *Brain activation*. New York: Wiley-Liss; 1993:341–364.
33. MacLean PD. Some psychiatric implications of physiological studies on frontotemporal portion of limbic system (visceral brain). *EEG Clin Neurophysiol* 1952;4:407–418.
34. Powell E, Hines G. The limbic system: an interface. *Behav Biol* 1974;12:149–164.
35. Mountz JM, Modell JG, Wilson MW, et al. Positron emission tomographic evaluation of cerebral blood flow during state anxiety in simple phobia. *Arch Gen Psychiatry* 1989;46:501–504.
36. Roland PE, Erikson L, Widen L, Stone-Elander S. Change in regional cerebral oxidative metabolism induced by tactile learning and recognition in man. *Eur J Neurosci* 1989;1:3–18.
37. Murray EA, Mishkin M. Relative contributions of SII and area 5 to tactile discrimination in monkey. *Behav Brain Res* 1984;11:67–83.
38. Kiloh LG. Pseudo-dementia. *Acta Psychiatr Scand* 1961;37:336–350.
39. Allen GV, Saper CB, Hurley KM, Cechetto DF. Organization of visceral and limbic connections in the insular cortex of the rat. *J Comp Neurol* 1991;311:1–16.
40. Roland PE. Cortical regulation of selective attention in man. A regional cerebral blood flow study. *J Neurophysiol* 1982;48:1059–1078.
41. Corbetta M, Miezin FM, Shulman GL, Petersen SE. Selective attention modulates extrastriate visual regions in humans during visual feature discrimination and recognition. *Ciba Found Symp* 1991;163:165–175.
42. Roland PE, Skinhoj E. Extrastriate cortical areas activated during visual discrimination in man. *Brain Res* 1981;222:166–171.
43. Mazziotta JC, Phelps ME, Carson RE. Tomographic mapping of human cerebral metabolism: subcortical responses to auditory and visual stimulation. *Neurology* 1984;34:825–828.
44. Fuster JM. Unit activity in prefrontal cortex during delayed-response performance: neural correlates of transient memory. *J Neurophysiol* 1973;36:61–78.
45. Kubota K, Iwamoto T, Suzuki H. Visuokinetic activities of primate prefrontal neurons during delayed-response performance. *J Neurophysiol* 1974;37:1197–1212.
46. Niki H, Watanabe M. Prefrontal unit activity and delayed response: relation to cue location versus direction of response. *Brain Res* 1976;105:79–88.
47. Kubota K, Funahashi S. Direction-specific activities of dorsolateral prefrontal and motor cortex pyramidal tract neurons during visual tracking. *J Neurophysiol* 1982;47:362–376.
48. Sawaguchi T, Matsumura M, Kubota K. Catecholaminergic effects on neuronal activity related to a delayed response task in monkey prefrontal cortex. *J Neurophysiol* 1990;63:1385–1400.
49. Murase S, Grenhoff J, Chouvet G, Gonon FG, Svensson TH. Prefrontal cortex regulates burst firing and transmitter release in rat mesolimbic dopamine neurons studied in vivo. *Neurosci Lett* 1993;157:53–56.
50. Pandya DN, Van Hoesen GW, Mesulam MM. Efferent connections of the cingulate gyrus in the Rhesus monkey. *Exp Brain Res* 1981;42:319–330.
51. Lassen NA, Andersen AR, Friberg L, Paulson OB. The retention of [^{99m}Tc]-d,l-HMPAO in the human brain after intracarotid bolus injection: a kinetic analysis. *J Cereb Blood Flow Metab* 1988;8:S13–S22.
52. Inugami A, Kanno I, Uemura K, et al. Linearization correction of ^{99m}Tc-labeled hexamethyl-propylene amine oxime (HMPAO) image in terms of regional CBF distribution: comparison to $C^{15}O_2$ inhalation steady-state method measured by positron emission tomography. *J Cereb Blood Flow Metab* 1988;8:S52–S60.
53. Yonekura Y, Nishizawa S, Mukai T, et al. SPECT with [^{99m}Tc]-d,l-hexamethyl-propylene amine oxime (HMPAO) compared with regional cerebral blood flow measured by PET: effects of linearization. *J Cereb Blood Flow Metab* 1988;8:S82–S89.
54. Heiss WD, Herholz K, Podreka I, Neubauer I, Pietrzyk U. Comparison of [^{99m}Tc]HMPAO SPECT with [^{18}F]fluoromethane PET in cerebrovascular disease. *J Cereb Blood Flow Metab* 1990;10:687–697.
55. Andersen AR, Friberg H, Kundsen KBM, et al. Extraction of [^{99m}Tc]-d,l-HMPAO across the blood-brain barrier. *J Cereb Blood Flow Metab* 1988;8:S44–S51.
56. Murase K, Tanada S, Inoue T, et al. Measurement of the blood-brain barrier permeability of ^{123}I-IMP, ^{99m}Tc-HMPAO and ^{99m}Tc-ECD in the human brain using compartment model analysis and dynamic SPECT [Abstract]. *J Nucl Med* 1991;32:P911.
57. Axelsson B, Msaki P, Israelsson A. Substraction of compton-scattered photons in single-photon emission computerized tomography. *J Nucl Med* 1984;25:490–494.
58. Jaszczak RJ, Greer KL, Floyd CE Jr, Harris CC, Coleman RE. Improved SPECT quantification using compensation for scattered photons. *J Nucl Med* 1984;25:893–900.
59. Ichihara T, Ogawa K, Motomura N, Kubo A, Hashimoto S. Compton scatter compensation using the triple-energy window method for single- and dual-isotope SPECT. *J Nucl Med* 1993;34:2216–2221.
60. Talairach J, Tournoux P. *Co-planar stereotaxic atlas of the human brain*. Stuttgart: Georg Thieme Verlag; 1988.